Deletion of the murine scavenger receptor CD68[s]

Li Song,[1],* Carolyn Lee,* and Christian Schindler[2],*

Departments Microbiology & Immunology* and Medicine,[†] Columbia University, New York, NY

Abstract Scavenger receptors (ScRs) are a structurally unrelated family of receptors with the ability to bind modified low density lipoprotein (LDL) as well as a broad range of polyanionic ligands. CD68, whose expression is restricted to mononuclear phagocytes, is a unique ScR family member, owing to its lysosome associated membrane protein (LAMP)-like domain and predominant endosomal distribution. Knockout (ko) mice were generated to directly evaluate the role murine CD68 may play in oxidized LDL (Ox-LDL) uptake. However, CD68$^{-/-}$ macrophages took up Ox-LDL robustly. Likewise, no defects were observed in the ability of CD68$^{-/-}$ mononuclear phagocytes to take up or mount an effective innate response against a number of microbes. Curiously, CD68$^{-/-}$ mononuclear phagocytes exhibited a trend toward enhanced antigen presentation to CD4+ T-cells, raising the possibility that CD68 may function either to negatively regulate antigen uptake, loading, or major histocompatibility complex class II (MHC-II) trafficking.—Song, L., C. Lee, and C. Schindler. **Deletion of the murine scavenger receptor CD68.** *J. Lipid Res.* 2011. **52:** 1542–1550.

Supplementary key words cholesterol uptake • macrophage • Ox-LDL • knockout MHC-II • antigen presentations • DC

CD68 and its murine homolog, macrosialin, is a highly glycosylated, ~95-110 kDa member of the lysosome-associated membrane protein (LAMP)-1 family, which is widely expressed on mononuclear phagocytes (1–3). It was initially identified as the antigen recognized by monoclonal antibodies directed against human and murine macrophage epitopes (2, 3). Immunohistochemical studies revealed that CD68 expression was largely restricted to monocytes and tissue-specific macrophages, notably including those in the peritoneum, lungs, spleen, and liver, as well as Langerhans cells and microglia (1, 4). Moreover, expression appeared to correlate with macrophage activation (5, 6). Consistent with these observations, the CD68 promoter has been exploited successfully to direct the expression of transgenes toward the macrophage lineage in vivo (7–9).

The characteristic pattern of expression on macrophages and a robust ex vivo affinity for oxidized low-density lipoproteins (Ox-LDL) (10) led to the classification of CD68 as a group D scavenger receptor (4, 11). Consistent with its classification as a LAMP-1 family member, CD68 was found to predominately localize to late endosomal and lysosomal compartments with a modest level of cell surface expression (12). Its short cytoplasmic tail, ability to rapidly traffic from cell surface to endosomes, and its intrinsic ability to bind Ox-LDL and phosphatidylserine, were often cited as evidence that CD68 served as a scavenger receptor (3, 10, 12, 13).

Although initially characterized for their ability to direct lipid and apoptotic cell uptake, the ability of scavenger receptors (ScRs) to recognize polyanionic ligands has also afforded them an important role in the nonopsonic phagocytosis of numerous microbes (1, 4). Consistent with this, a number of single and double murine ScR knockouts (ko) have validated their roles in these seemingly disparate inflammatory processes (1, 4). Although CD68 shares a number of these features, more recent studies have called into question its role in the recognition and uptake of Ox-LDL (14). Rather, they raised the possibility that CD68 may regulate the response to ligands after internalization. To more carefully explore the potential role CD68 plays in the ability of macrophages to either take up or direct an innate response to Ox-LDL and microbial ligands, knockout mice were generated. Analysis of CD68$^{-/-}$ mononuclear phagocytes failed to support an important

Abbreviations: BAL, broncho-alveolar lavage; BM, bone marrow; BMDC, bone marrow-derived dendritic cell; BMM, bone marrow-derived macrophage; CFU, colony-forming unit; DAMP, danger-associated molecular pattern; DC, dendritic cell; DT, diphtheria toxin; FACS, fluorescent activated cell sorting; IL, interleukin; ko, knockout; LAMP-1, lysosome-associated membrane protein-1; LPS, lipopolysaccharide; MEF, murine embryonic fibroblast; Mϕ, macrophage; MOI, multiplicities of infection; NO, nitric oxide; OVA, ovalbumin; Ox-LDL, oxidized LDL; MHC-II, major histocompatibility complex class II; PAMP, pathogen-associated molecular pattern; PEC, peritoneal-elicited cell; PFU, plaque-forming unit; ScR, scavenger receptor; TNF, tumor necrosis factor; VSV, vesicular stomatitis virus; wt, wild-type.

[1] Current address of L. Song: Division of Rheumatology, Hospital for Special Surgery, New York, NY.

[2] To whom correspondence should be addressed.
 e-mail: cws4@columbia.edu (C.S.)
[s] The online version of this article (available at http://www.jlr.org) contains supplementary data in the form of five figures.

role in the uptake of either Ox-LDL, microbes, or an associated inflammatory response. However, the enhanced capacity of these knockout cells to present antigen to CD4^{+} T-cells raises the possibility that CD68 may negatively regulate major histocompatibility complex class II (MHC-II) activity.

MATERIALS AND METHODS

Gene targeting

CD68 gene targeting vector was generated by PCR amplification (Expanded Long Template PCR System; Roche, Indianapolis, IN) of a 1.6 kb short arm and 6.5 kb long arm from C57Bl6/J mice genomic DNA, as illustrated in Fig. 2, with primers: 5′ TGC GGC CGC CCC TAT GCT GAA ACC CAA GTG TTC C 3′ and 5′ CTC TAG ACA TAT GAG AGA TGC TCA GAC CAG CTA GGC 3′ for the short arm and 5′ CTC GAG CGG CTC CCT GTG TGT CTG ATC TTG C 3′ and 5′ GCG GCC GCA GGA CAG GGG CTA CAC AGA AAC CC 3′ for the long arm (Not I, Xba I, Nde I, Xho I, and Not I endonuclease restriction sites are underlined and were included for cloning; New England Biolab, MA). A loxP-flanked neomycin cassette was amplified from pMC1neo Poly A plasmid (Stratagene, San Diego, CA) with primers: 5′ CTC GAG ATA ACT TCG TAT AGC ATA CAT TAT ACG AAG TTA TGA ACA AAC GAC CCA ACA CCC GTG C 3′ and 5′ GTC GAC ATA ACT TCG TAT AAT GTA TGC TAT ACG AAG TTA TGC AGT GTG GTT TTG CAA GAG GAA GC 3′ (Xho I and Sal I enoduclease restriction sites are underlined) and cloned, inverted, downstream from an rtTA cassette (15). This unit was then cloned immediately downstream and in frame with the CD68 initiation ATG located at the 3′ end of the short arm. The targeting construct was assembled in a vector provided by Dr. V. Lin that features a negative selectable diphtheria toxin (DT) gene (16). The integrity of the targeting construct was confirmed by sequencing prior to electroporation into 129 R1 ES cells (17). Neomycin resistant clones were evaluated by Southern blotting with a probe localized to the 5′ end of the short arm (see Fig. 2). Properly targeted CD68 knockout ES cells (2 of 192 neomycin-positive clones) were introduced into blastocyts to generate chimeric mice, as previously reported (18). Chimeric mice were either crossed with 129 mice or backcrossed seven generations to the C57Bl/6J background. Transmission of the knockout allele was determined by Southern blot and PCR. Columbia University review committees approved all relevant studies.

Cell culture

Resident peritoneal macrophages were harvested by lavage with 10 ml RPMI 1640 (Invitrogen-GIBCO, Grand Island, NY) supplemented with 10% FCS (Hyclone, Logan, UT) from freshly euthanized mice. Recovered cells were plated (1×10^6 cells/ml), and nonadherent cells were removed after 2 h by aspiration. Peritoneal-elicited cells (PEC; i.e., macrophages) were recovered by the same procedure four days after instillation of 1 ml of 4% thioglycollate (DIFCO; Voigt Global Dist., Inc, Lawrence, KS). Bone marrow-derived macrophages (BMMs) were prepared in RPMI 1640 supplemented with 10% FCS, penicillin/streptomycin (GIBCO), and 20% L-cell conditioned media, as previously reported (19). Bone marrow-derived dendritic cells (BMDC) were prepared similarly, except that they were grown in RPMI 1640 supplemented with a 1/30 dilution of GM-CSF conditioned media (from J558 cells), 5% FCS, pen/strep, and β-mercaptoethenol (GIBCO), as previously described (20). Cells were fed gently with fresh media on days 3 and 5. On day 7, loosely adherent clustering dendritic cells (DC) were recovered (∼75% CD11c^{+}) and replated for an additional two or three days prior to analysis. Phagocytic activity was measured by incubating macrophages with either heat-killed FITC-labeled *S. aureus* as previously described (21); or LDL (Intracel Resources, Frederick, MD) that had been moderately oxidized with 40 μM CuSO$_4$ as previously reported (22). Lipid uptake was measured by flow cytometry of live cells by gating on DiI (1,1′-dioetadeeyl-3,3,3′,3′-tetramethylindocarboeyanine perchlorate; Sigma-Aldrich, St. Louis, MO) labeled Ox-LDL, or in fixed PECs by staining with oil red O, as previously reported (22, 23). PECs were also stained with antibodies specific for CD68 (1:100, 2 h; MAC1957; FA11; Serotec, Oxford, UK) and LAMP-1 (Southern Biotech, Birmingham, AL) after samples had been fixed (4% paraformaldehyde, methanol; 20 min) and blocked (2% goat serum) as previously reported (24, 25). Antibodies were detected with anti-rat IgG-FITC (1:100, 1 h; STAR69, Serotec) or anti-rat IgG-Cy3 (1:500, 1 h; Jackson ImmunoResearch, West Grove, PA) or anti-rat IgG-HRP (Vector Labs, Burlingame, CA) and visualized with a DAB substrate kit from Vectastain (Vector Labs) (23). Images were captured with a Nikon Eclipse TE300 microscope on a Spot camera (Sterling Heights, MI) and analyzed with OpenLabs (Waltham, MA) software.

Microbicidal activity

The ability of macrophages to generate nitric oxide (NO) in response to treatment with lipopolysaccharide (LPS) (100 ng/ml; from *E. coli* serotype 055:B5; Sigma-Aldrich, St. Louis, MO) and/or IFN-γ (50 U/ml; murine; PBL, Piscataway, NJ) was carried out as previously reported (24). Growth of *Legionella pneumophila*, a facultative intracellular bacterium, was evaluated by infecting BMMs (0.5×10^6 per well in a 12-well plate, in triplicate) with 3,000 colony-forming units (CFU) of postlogarithmic growth bacteria, as recently reported (26). The capacity of macrophages to promote viral growth was evaluated by infecting BMMs with vesicular stomatitis virus (VSV; Indiana strain) at multiple multiplicities of infections (MOI) and titering the supernatant for plaque-forming units (PFU) on Vero cells, as previously reported (24).

Flow cytometry

Fluorescence activated cell sorting (FACS) analysis was carried out on cells harvested from euthanized mice. Broncho-alveolar lavage (BAL) fluid was recovered in three sequential 1 ml (PBS) lung lavages, as reported (27, 28). Bone marrow (BM) and peritoneal macrophages were prepared as described above. Additional leukocytes were harvested from femurs (BM cells) and spleen (splenocytes), or blood. Single-cell suspensions were RBC-depleted (Sigma), resuspended in RPMI 1640/10% FCS, and then counted and/or stained for FACS. Adherent cells (BMMs) were treated for 5 min with trypsin/EDTA (Sigma-Aldrich), whereas BMDCs were collected by gentle pipetting prior to staining for FACS. Cells were stained with anti-CD11b (M1/70), F4/80 (BM8), Gr-1 (RB6-8C5), CD8a (53-6.7), CD206 (48-2069) from eBioscience (San Diego, CA) or anti-CD11c (HL3), CD3e (145-2C11), CD4 (RM4-5), I-Ab (MHC-II; AF6-120.1), CD86 (GL1), NK1.1 (PK136) from BD Pharmingen (San Diego, CA) or anti-CD68 (MAC1957; FA11) and CD206 (MR5D3) from Serotec (Oxford, UK), after treatment with Fc-blocker (anti-CD16/CD32, 2.4G2; BD-Pharmingen). Cells were fixed and stained with CD68 antibodies as per manufacturer (Serotec). Data were acquired on a FACS Calibur or FACS LSR-II (Beckton Dickinson, Franklin Lakes, NJ) and analyzed by FlowJo software (TreeStar, Ashland, OR).

Cytokine profiling

Cultured macrophages or DCs were treated with LPS (100 or 1,000 ng/ml; Sigma), IFN-γ (50 U/ml; murine; PBL, Piscataway,

NJ), interleukin (IL)-4 (10 ng/ml; Peprotech, Rocky Hill, NJ), zymosan (100 µg/ml; Sigma) or silicates (0.4 mg/ml; see below). Supernatants were collected after 24 h and evaluated by ELISA for tumor necrosis factor (TNF)-α and IL-6 production (eBioscience) or IL-1β production (Pierce, Rockford, IL). Quartz (Min-U-Sil 5) was a gift from US Silica (Berkeley Springs, WV) and featured >98% purity, an average size of 1.83 µm (range 1.70-1.89 µm), and no amorphous coating (29, 30). Tridymite (99% purity, 0.5-1 µm, no amorphous coating) was a generous gift from B. Pernis (31, 32). Silicates, which were baked at 250°C for 16 h prior to suspension in PBS, were sonicated prior to stimulation and negative for endotoxin contamination (Limulus assay; Cambrex Bio Science, Walkersville, MD).

T-cell analysis

An amount of 3×10^5 ovalbumin (OVA)-specific CD4$^+$ T-cells (anti-CD4 MACS beads; Miltenyi Biotech, Auburn, CA) from OT-II TCR transgenic spleens were cultured for four days with 3×10^4 BMDCs, which had previously been loaded for 4 h with increasing concentrations of OVA (Worthington Biochemical Corporation, Lakewood, NJ) or OVA peptide 326-332 (New England Peptide, Inc., Gardner, MA). T-cell proliferation was measured by ^{3}H-thymidine incorporation (14 h, 37°C; Perkin Elmer Life Sciences, Shelton, CT), as previously reported (20).

PCR

DNA or RNA was recovered from FACS-purified leukocyte populations with Trizol (Invitrogen). RNA was reverse transcribed with SuperScript™ II (Invitrogen), as previously reported (19, 24). DNA and cDNA were either PCR amplified by standard or quantitative methods (ABI Prism 7700 with SYBR green master mix; Applied Biosystems, Foster City, CA). Gene expression was normalized to a β-actin or 18S rRNA control. Ct values and standard curves were generated by plotting log of DNA concentration versus Ct values from 1:5 serial dilutions with SDS1.9.1 software (Applied Biosystems). Primers were annealed at 60 C and run 40 cycles. Primers sets included: Arginase-1 (forward) 5′ aga cca cag tct ggc agt tg, (reverse) 5′ cca ccc aaa tga cac ata gg; 18S (forward) 5′ tca aga acg aaa gtc gga gg 3′, (reverse) 5′ gga cat cta agg gca tca ca 3′; eif4a1 (forward) 5′ gga agg cgt cat cga gag taa ctg, (reverse) 5′ ccc aat gca ggc atg aca aag agg; mupd.1 (forward) 5′ gcg ctg ttc ctg aca ctc cag acc, (reverse) 5′ cca gta gaa gag gac ctg ggc agc.

RESULTS

Characterization and deletion of CD68

Although predominately restricted to endosomes, CD68 expression has been largely associated with myeloid cells from the macrophage lineage (1). Consistent with previous reports, CD68 staining was strongest after membrane permeablization, and it was largely localized to LAMP1-positive vesicles (supplementary Fig. I) (1). When primary murine myeloid cells were evaluated, strong CD68 expression was observed in several macrophage lineages, including alveolar, splenic, BM, and peritoneal macrophages, as well as BM culture-derived macrophages (see **Fig. 1**) (1, 33). Likewise, robust CD68 expression was observed in several DC populations, including pulmonary- and splenic-CD8α$^+$ DCs and BM culture-derived DCs, but not in CD8α$^-$ DCs (Fig. 1). As anticipated, CD68 was not detected on B220$^+$ or CD3$^+$ lymphocytes (not shown).
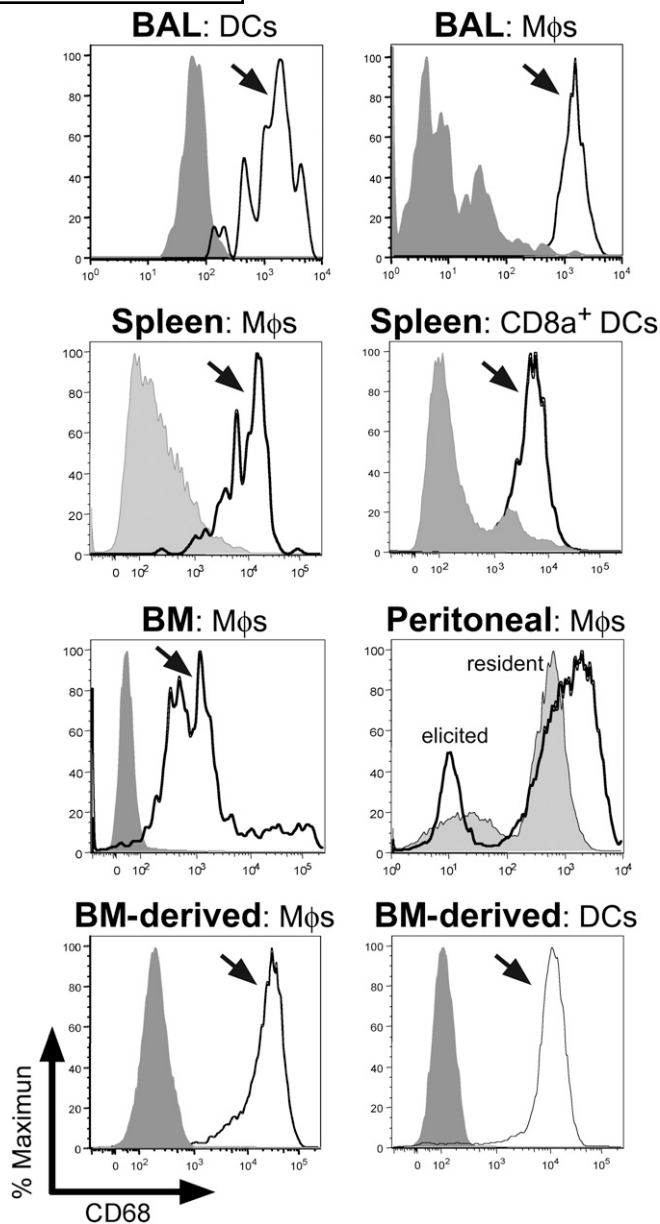
Fig. 1. CD68 expression in murine mononuclear phagocytes. Primary, as well as BM-derived, macrophages and DCs were stained for specific cell surface markers and CD68, and then evaluated by FACS. CD68 expression was high in BAL DCs (CD11b$^+$/CD11c$^+$ versus CD11b$^+$/CD11c$^-$ in gray) and Mφs (CD11b$^-$/CD11c^{++} versus CD11b$^-$/CD11c$^-$ in gray). CD68 expression was also robust in splenic Mφs (CD11b$^+$/F4/80$^+$ versus CD11b$^-$/F4/80$^-$ in gray) and lymphoid DCs (CD11c$^+$/MHC-II$^+$/CD8α$^+$ versus CD11c$^+$/MHC-II$^+$/CD8α$^-$ in gray). Likewise, CD68 expression was strong in Mφs recovered from BM (CD11b$^+$/F4/80$^+$ versus unstained in gray), as well as resident (CD11b$^+$/F4/80$^+$ in gray) and thioglycollate-elicited (CD11b$^+$/F4/80$^+$ black line) Mφs. Finally, CD68 expression was also elevated in BM-derived Mφs (CD11b$^+$ versus unstained in gray) and BM-derived DCs (CD8$^+$/CD11c$^+$ versus unstained in gray).

To explore the potential role CD68 plays in ligand uptake, its gene was targeted for deletion by a recombination vector featuring two homology arms and a neomycin cassette (see **Fig. 2**). Chimeric mice with a targeted allele were then either crossed with 129 or C57Bl/6 mice and then
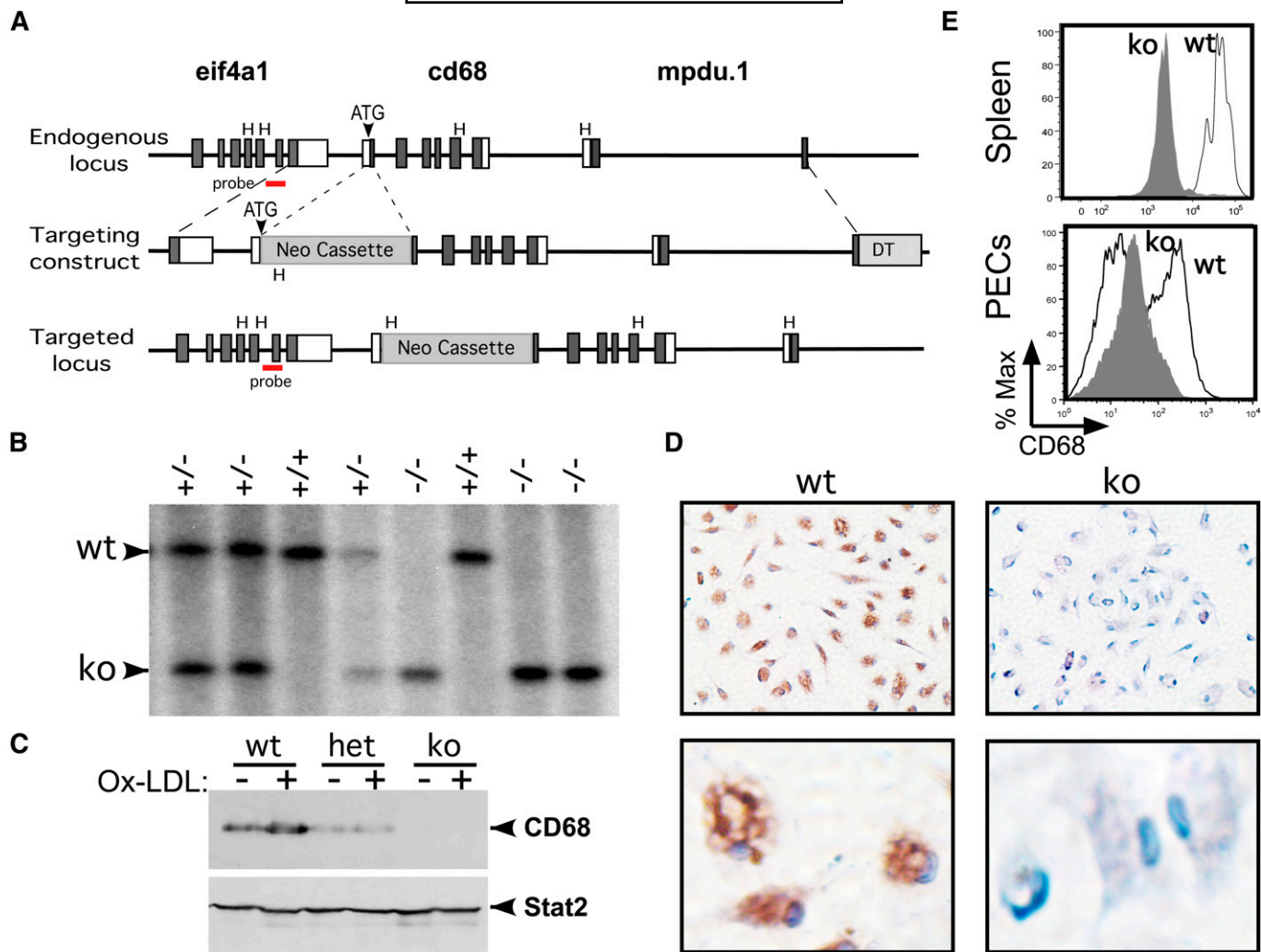
Fig. 2. Generation of CD68 knockout mice. (A) Three models describe: *i*) the endogenous *cd68* locus, which lies in a gene-rich cluster - *eif4a1* (eukaryote initiation factor 4A1) abuts the promoter and *mpdu.1* (Mannose-P-dolichol utilization defect 1) lies downstream; *ii*) the cd68 gene-targeting vector featuring a 1.6 kb 5′ homology arm, a Neo cassette, a 6.5 kb 3′ homology arm, and the DT gene; and *iii*) the targeted locus. Exons are illustrated as rectangles (dark = coding; white = noncoding). Hind III (H) restriction sites and the CD68 initiation codon (ATG) are indicated. Neomycin resistance (Neo) (including loxP sites and rtTA; not shown) and DT gene cassettes are depicted as gray rectangles. 5′ "outside" probe used for Southern blots lies in *eif4a1*, as shown. (B) Southern blotting analysis of progeny from a het$^{+/-}$ intercross. Tail DNA was digested with Hind III and analyzed with the 5′ probe. The wt$^{+/+}$ and targeted (ko)$^{-/-}$ bands are marked. (C) Western blot of whole-cell extracts from PECs. Whole-cell extracts from wt, heterozygous (het) and ko PECs were loaded, or not, with Ox-LDL (100 μg/ml, 16 h), fractionated by SDS-PAGE, and immunoblotted with an antibody specific for CD68 (FA11; Serotec). The filter was reprobed for Stat2 as a loading control. (D) Immunohistochemical stain of wt and ko PECs from panel C stained for CD68 (brown color) at 10× (upper panels) and 60× (lower panels) magnification. Cells are counterstained with hematoxylin (blue). (E) FACS analysis for CD68 expression of wt and ko splenic macrophages and PECs, as in Fig. 1.

interbred to homozygosity. Progeny CD68 knockout (CD68$^{-/-}$) mice developed with normal Mendelian genetics in both backgrounds (e.g., Fig. 2B; data not shown); they exhibited no obvious phenotypes, including no evidence of organomegally and no significant perturbations of defined leukocyte populations in either the blood or spleen (**Tables 1** and **2**; supplementary Fig. II). Western blotting, immunohistochemical studies, and FACS analysis confirmed an absence of CD68 expression in macrophages from CD68 knockout mice (Fig. 2C–E). CD68$^{+/-}$ (i.e., heterozygous) mice exhibited a corresponding partial decrease in CD68 expression (Fig. 2C). Given the relatively high density of genes at the CD68 locus, it was important to confirm that the expression of both *eif4a1* and *mpdu.1*

(upstream and downstream flanking genes; see Fig. 2) was not affected by the introduction of a neomycin cassette into the CD68 locus (supplementary Fig. III). In summary, these studies revealed that homozygous deletion of the CD68 gene was not associated with any significant developmental or homeostatic defects.

CD68$^{-/-}$ macrophages exhibit normal scavenger receptor activity

Shortly after its initial characterization (3, 34), CD68 was identified as a 94-97 kDa receptor for Ox-LDL, adding it to the growing family of scavenger receptors (1, 4). Despite its largely intracellular distribution, dynamic studies suggested CD68 exhibited a robust capacity to rapidly transport

TABLE 1. Leukocyte subtypes in CD68$^{-/-}$ blood

	B220$^+$	CD3$^+$	CD11b$^+$; Gr-1^{hi}	CD11b$^+$; Gr-1^{lo}	CD11b$^-$; Gr-1$^+$
wt	44.9 ± 3.9	27.2 ± 3.9	4.4 ± 2.3	6.8 ± 0.4	2.3 ± 0.1
het	41.4 ± 3.8	26.8 ± 4.8	3.9 ± 0.6	7.5 ± 0.6	2.2 ± 0.1
ko	44.1 ± 5.5	20.4 ± 1.7	8.1 ± 3.2	6.3 ± 0.8	2.4 ± 0.5

Peripheral blood from three-month-old matched wild-type (wt), heterozygous (het), and CD68$^{-/-}$ (ko) mice that were backcrossed to C57Bl/6J mice six times, was stained for B220 (B lymphocytes), CD3 (T lymphocytes), CD11b (macrophages), and Gr-1 (granulocytes/monocytes) and analyzed by FACS. Mean and standard deviation of the percentage of positive cells are shown.

Ox-LDL as well as other ligands into the endosomal compartment (12). Subsequent RNAi knockdown studies, however, failed to confirm a significant role for CD68 in Ox-LDL uptake (14). To more rigorously explore the capacity of CD68 to serve as a scavenger receptor, primary peritoneal macrophages were harvested from knockout mice and incubated with increasing concentrations of Ox-LDL. Both wild-type and knockout macrophages took up Ox-LDL in a dose-dependent manner (**Fig. 3A**, B; supplementary Fig. IV). Intriguingly, CD68$^{-/-}$ macrophages even exhibited a trend toward enhanced Ox-LDL uptake at lower doses. Next, the more general phagocytic activity of CD68 knockout macrophages was evaluated by incubating cells with fluorescently-labeled, heat-killed *Staphylococcus aureus.* Again, CD68$^{-/-}$ macrophages exhibited a dose-dependent uptake of bacteria that paralleled the pattern observed in wild-type macrophages (Fig. 3B, top panels). Moreover, CD68$^{-/-}$ macrophages exhibited no significant differences in either the binding (i.e., 4°C) or uptake (i.e., 37°C) of opsonized, labeled, heat-killed *S. aureus* (Fig. 3B, bottom panels), suggesting that CD68 does not play an important role in either Ox-LDL or bacteria uptake by macrophages.

Innate immune response in CD68$^{-/-}$ macrophages

Since CD68 is predominately localized to the endosomal compartment, its capacity to contribute to the innate intracellular response to microbial pathogens was explored. First, the capacity to generate NO, an important antibacterial effector, was evaluated (35). As shown in **Fig. 4A**, both wild-type (wt) and CD68$^{-/-}$ macrophages produced equivalent quantities of NO in response to stimulation with IFN-γ and LPS. Next, the capacity of CD68 to affect the innate response to microbial infection was evaluated. Consistent with previous studies on the innate response, when murine macrophages were infected with *L. pneumophila,* they replicated modestly over a four-day period (Fig. 4B)

TABLE 2. Leukocyte distribution in CD68$^{-/-}$ spleen

	B220$^+$	CD3$^+$	CD11b$^+$	CD11c$^+$
wt	61.1 ± 1.7	25.1 ± 3.2	4.3 ± 3.9	2.3 ± 1.8
het	58.3 ± 5.0	25.4 ± 2.4	4.3 ± 2.3	2.4 ± 1.0
ko	59.8 ± 1.7	25.5 ± 2.7	3.8 ± 1.2	1.8 ± 0.7

Splenocytes from three-month-old matched wild-type (wt), heterozygous (het), and CD68$^{-/-}$ (ko) mice (as in Table 1) were stained for B220 (B lymphocytes), CD3 (T lymphocytes), CD11b (macrophages), and CD11c (dendritic cells) and analyzed by FACS. Mean and standard deviation of the percentage of positive cells are shown.
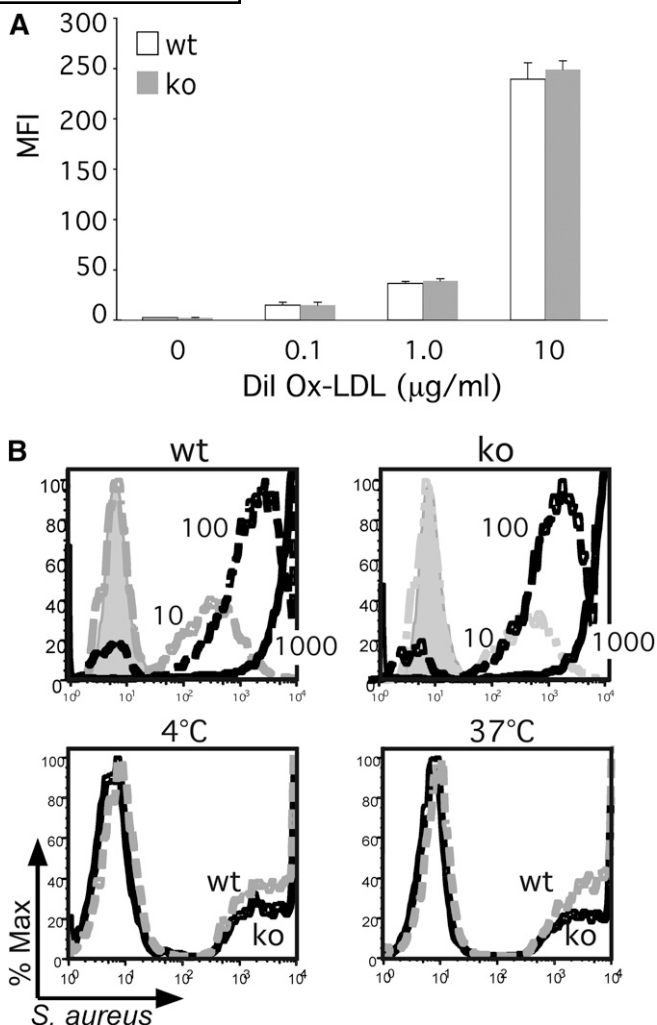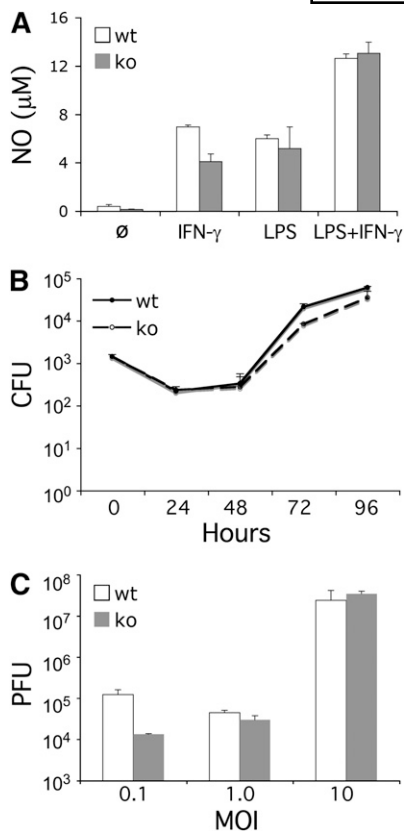
Fig. 3. CD68 knockout macrophages exhibit robust phagocytic activity. (A) wt and CD68 ko PECs were loaded with increasing doses of DiI-labeled Ox-LDL (0.1, 1.0, and 10 μg/ml, 4 h, 37°C) as indicated. Lipid uptake was measured by FACS and graphed as mean fluorescence intensity (MFI). (B) In the top panels, wt and ko PECs were incubated with increasing MOIs (10 - dotted gray lines; 100 - dotted black lines; 1000 - solid black lines) of FITC-labeled, heat-killed *Staphylococcus aureus* for 4 h, and then evaluated by FACS. Extracellular fluorescence was quenched with trypan blue. Histogram of maximal fluorescence reveals an equivalent, dose-dependent bacterial uptake by wt and ko PECs. Untreated cells are shown in gray. The bottom panels demonstrate that after 30 min, opsonized (mouse serum) FITC-*S. aureus* (MOI = 10) are both bound (i.e., 4°C) and taken up (37°C) equivalently in wt (dotted gray lines) and ko (solid black lines) PECs.

(26, 36). More importantly, wt and CD68$^{-/-}$ macrophages supported equivalent levels of growth, suggesting CD68 does not significantly contribute to the innate response toward these intracellular pathogens. Similarly, CD68$^{-/-}$ macrophages and mice both failed to exhibit a defective innate response upon infection with *Listeria monocytogenes,* another intracellular bacterial pathogen (data not shown). Next, the capacity of CD68$^{-/-}$ macrophages to support the growth of vesicular stomatitis virus was evaluated. Again, there were no significant differences in VSV replication in either wt or CD68$^{-/-}$ macrophages. This was true
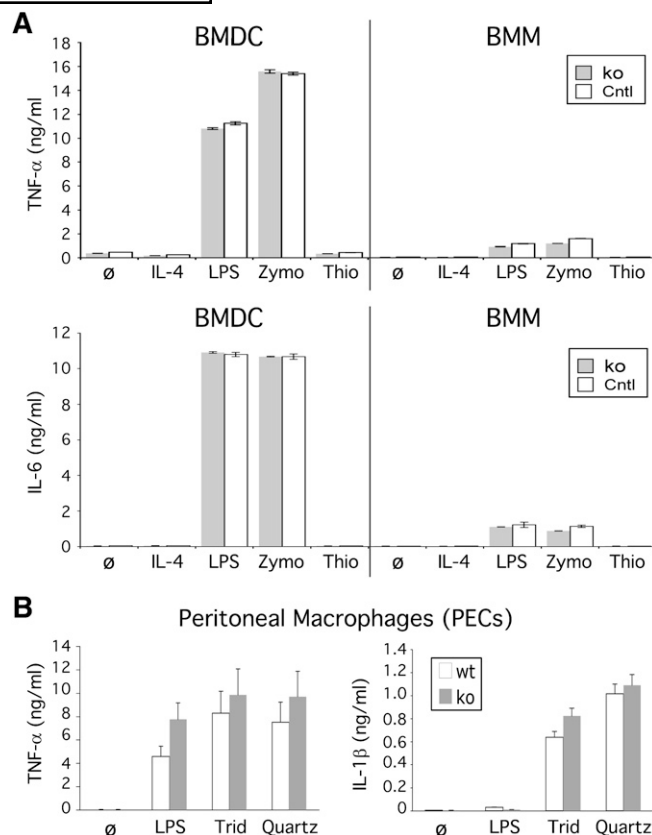
Fig. 4. CD68 knockout macrophages exhibit a normal response to microbial infection. (A) IFN-γ (50 U/m, 48 h) and LPS (100 ng/ml, 48 h) stimulated equivalent levels of NO production in wt and ko PECs. (B) wt and ko BMMs yielded equivalent levels of *L. pneumophila* growth (CFUs) over four days (26). (C) wt and ko BMMs yielded equivalent levels of VSV (PFUs) at several MOIs (0.1, 1.0, and 10; 48 h).

Fig. 5. CD68 knockout mononuclear phagocytes exhibit a normal inflammatory response. (A) Control (Cntl; wt and het) and ko BMDCs (day 9) and BMMs produce equivalent levels of TNF-α and IL-6 after 16 h of stimulation with LPS (100 ng/ml) or Zymosan (Zymo; 100 μg/ml). Stimulation with IL-4 (10 ng/ml) and thioglycollate (Thio; 2 mg/ml) served as negative controls. (B) Control (Cntl; wt and het) and ko PECs produce equivalent levels of TNF-α and IL-1β after 16 h stimulation with Tridymite (Trid; 0.4 mg/ml) or Quartz (0.4 mg/ml).

at both low MOIs, which feature a more robust innate response, and at the higher MOIs favoring more robust viral growth (Fig. 4C).

The inflammatory response of CD68$^{-/-}$ mononuclear phagocytes

In addition to their phagocytic capacity, mononuclear phagocytes feature a number of innate immune receptors that detect pathogen-associated molecular patterns (PAMP; e.g., LPS and zymosan) (37) and danger-associated molecular patterns (DAMP; e.g., silica) (30, 38), which direct the secretion of potent inflammatory cytokines (e.g., TNF-α, IL-1β, and IL-6). To examine whether CD68 might contribute to this response, CD68$^{-/-}$ macrophages and DCs were stimulated with a few PAMPs and DAMPs. No differences were observed in the capacity of either LPS or Zymosan to stimulate TNF-α or IL-6 production in either wild-type or CD68$^{-/-}$ macrophages or DCs (**Fig. 5A**). Moreover, the robust inflammatory response of CD68$^{-/-}$ macrophages to LPS (Fig. 5A) and IFN-γ (data not shown) indicated that CD68 does not play a significant role in the response of classically activated M1 macrophages. Likewise, no differences were observed in the ability of CD68$^{-/-}$ macrophages to be polarized to the M2 noninflammatory phenotype, which is characterized by CD206, arginase 1, and IL-10 expression (supplementary Fig. V) (39).

Next, we examined the ability of CD68$^{-/-}$ macrophages to respond to silica crystals (e.g., quartz), which have recently been shown to robustly stimulate IL-1β secretion through activation of the inflammasome (30, 32, 38). Wild-type and CD68$^{-/-}$ peritoneal macrophages were stimulated with two forms of highly purified, endotoxin-free crystalline silica, tridymite, and quartz. Again, the response of CD68$^{-/-}$ macrophages was equivalent to wt macrophages (Fig. 5B). Additional studies confirmed that these responses were sensitive to cytochalasin D (data not shown), suggesting these crystals must enter the cell to be sensed (30, 38). In summary, these studies revealed that CD68 does not significantly contribute to the innate response to a divergent set of inflammatory stimulants.

Adaptive immunity in CD68$^{-/-}$ mononuclear phagocytes

Having excluded an important role for CD68 in either the uptake or inflammatory responses associated with innate immunity, the possibility that CD68 might play a role in adaptive immunity was explored. Because of their potent capacity to present antigens, these studies focused on

DCs. First, PAMP-dependent upregulation of MHC-II and coreceptors was examined. These studies highlighted a modest increase in basal MHC-II, but not CD86, surface expression in CD68$^{-/-}$ BMDCs (**Fig. 6A**). However, the robust, LPS-dependent induction of MHC-II was essentially equivalent in wt and CD68$^{-/-}$ DCs. CD86 upregulation was modestly enhanced in CD68$^{-/-}$ DCs.

Next, DCs were loaded with increasing doses of OVA to evaluate their ability to present antigen to OVA-MHC-II-specific OT-II T-cells. At lower, nonsaturating concentrations of OVA, wt and CD68$^{-/-}$ DCs were equivalent in their capacity to stimulate proliferation of naïve OT-II T-cells (Fig. 6B). Yet at higher, but not the highest, concentration of OVA (i.e., 0.05 and 0.1 mg/ml; Fig. 6B) CD68$^{-/-}$ DCs exhibited increased ability to stimulate T-cell proliferation. Similarly, CD68$^{-/-}$ DCs loaded with a specific OT-II-activating OVA peptide stimulated more robust T-cell proliferation at higher doses (Fig. 6B). These observations raised the possibility that CD68 may negatively regulate the capacity of DCs to present antigen to naïve T-cells, especially under conditions of high antigen load.

DISCUSSION

CD68 is a member of the ScR family that has been widely exploited as a macrophage marker (reviewed in Refs. 1, 4, and 11). However, consistent with its conserved "extracellular" LAMP domain, CD68 predominately localizes to LAMP-1-positive intracellular vesicles. Expression is upregulated in response to various inflammatory stimuli, including oxidized LDL. Yet, despite robust binding activity, CD68's role in either the endocytosis or processing of oxidized LDL remains controversial (3, 10, 12–14). To more rigorously evaluate the role of this conserved member of the LAMP-1 family in inflammatory responses, CD68 knockout mice were generated. Initial characterization of tissues from CD68$^{-/-}$ mice underscored a loss of expression in both macrophage and DC populations that normally express CD68. Moreover, this was not associated with a perturbation in either the number or distribution of any leukocyte populations recovered from the blood, spleen, peritoneum, lung, or lymph nodes.

With a robust affinity for Ox-LDL and phosphatidylserine, initial studies had implicated CD68 in modified lipid uptake (12, 40). However, subsequent ectopic overexpression and partial knockdown studies failed to support an important role for CD68 in Ox-LDL uptake (14). Consistent with these observations, CD68$^{-/-}$ peritoneal macrophages (Fig. 3; supplementary Fig. IV) and BMMs (data not shown) failed to exhibit any defect in Ox-LDL uptake. Rather, several experiments revealed a trend toward enhanced lipid uptake in CD68$^{-/-}$ macrophages.

Having excluded an important role in Ox-LDL uptake, it was important to determine whether CD68 might direct the uptake of bacteria, a property associated with other ScRs. However, CD68$^{-/-}$ macrophages were fully able to bind and phagocytose both nonopsonized and opsonized
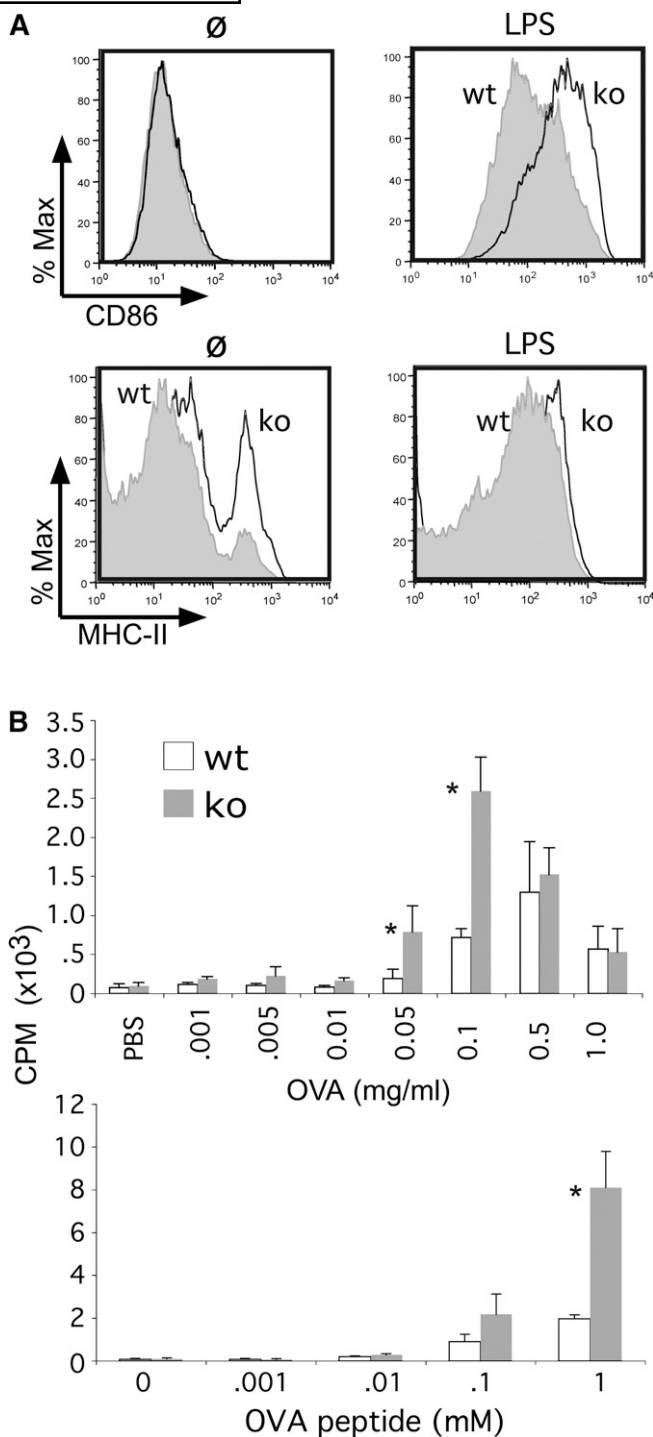
Fig. 6. CD68 knockout DCs exhibit enhanced antigen presenting activity. (A) LPS (100 ng/ml, 24 h) stimulated CD86 and MHC-II expression was evaluated in wt and ko BMDCs (day 9) by FACS. (B) OT-II T-cells were either stimulated with ovalbumin (OVA; 0.001-1.0 mg/ml, 4 h; top panel) or OVA-peptide (OVAp; 0.001-1.0 mM, 4 h; bottom panel) loaded wt and ko BMDCs (day 6). T-cell proliferation was measured by ^{3}H-Tdr incorporation, as previously reported (20). *P* values were 0.0019 for 0.01 mg/ml OVA, 0.0425 for 0.05 mg/ml OVA, 0.00196 for 0.1 mg/ml of OVA, 0.0946 for 0.1 mM OVAp, and 0.0451 for 1 mM OVAp.

S. aureus (Fig. 3B). Likewise, CD68$^{-/-}$ macrophages (see Fig. 4) and mice (data not shown) exhibited a normal innate response to infection with bacterial pathogens (e.g., *S. aureus* and *L. monocytogenes;* data not shown) and VSV. These observations are consistent with the possibility that CD68 may play a redundant role in phagosome-lysosome fusion, as has recently been reported in LAMP-1/LAMP-2 double-knockout murine embryonic fibroblasts (MEFS) (41). This potentially redundant role will be explored in future studies.

Next, we considered the possibility that CD68 might regulate other aspects of the immune response. First, the ability of a few signature PAMPs and DAMPs to stimulate an inflammatory response in either macrophages or DCs was evaluated. Again, the loss of CD68 was not associated with any defect in cytokine production (Fig. 5), but there was a trend toward modestly enhanced DC activation (i.e., cell surface CD86 and MHC-II expression) in CD68$^{-/-}$ mononuclear phagocytes. Consistent with a potential role in regulating the ability of these cells to present antigens, OVA-loaded CD68$^{-/-}$ DCs were found to be more effective in stimulating the proliferation of OVA-MHC-II-specific, OT-II T-cells, especially at higher doses of this antigen (Fig. 6). The equally enhanced capacity of CD68$^{-/-}$ DCs to present ovalbumin peptide to OT-II T-cells suggests that CD68 is not likely to regulate antigen processing but, rather, MHC-II loading or transport or both to the cell surface. Intriguingly, LAMP-1 and LAMP-2 may regulate Rab7-dependent phago-lysosomal interactions and trafficking (41). Moreover, LAMP-2 has been implicated in the "retrograde" movement of MHC-II molecules from a late-endosome/lysosome-like, multivesicular body, where they are stored and loaded with antigen into CD68-positive tubular structures, from which antigen-loaded MHC-II vesicles appear to bud on their way to the cell surface (42, 43). Consistent with the possibility that CD68 may negatively regulate this process, basal MHC-II surface expression was enhanced in CD68$^{-/-}$ DCs. However, this enhanced capacity to present antigens in vitro was not associated with a proclivity toward autoimmunity (aged CD68$^{-/-}$ mice remained healthy) or an overly exuberant innate response to bacterial infection. Future studies will need to more rigorously evaluate the potential role CD68 plays in regulating the complicated movement of MHC-II molecules from multivesicular bodies, where they are antigen-loaded, to the cell surface, where they present antigen. This investigation will include exploring whether loss of CD68 is associated with changes in either the quantity or quality of adaptive T-cell-dependent responses, as well as humoral immunity during controlled immune challenges.▪

REFERENCES

1. Taylor, P. R., L. Martinez-Pomares, M. Stacey, H. H. Lin, G. D. Brown, and S. Gordon. 2005. Macrophage receptors and immune recognition. *Annu. Rev. Immunol.* **23:** 901–944.
2. Micklem, K., E. Rigney, J. Cordell, D. Simmons, P. Stross, H. Turley, B. Seed, and D. Mason. 1989. A human macrophage-associated antigen (CD68) detected by six different monoclonal antibodies. *Br. J. Haematol.* **73:** 6–11.
3. Holness, C. L., R. P. da Silva, J. Fawcett, S. Gordon, and D. L. Simmons. 1993. Macrosialin, a mouse macrophage-restricted glycoprotein, is a member of the lamp/lgp family. *J. Biol. Chem.* **268:** 9661–9666.
4. Moore, K. J., and M. W. Freeman. 2006. Scavenger receptors in atherosclerosis: beyond lipid uptake. *Arterioscler. Thromb. Vasc. Biol.* **26:** 1702–1711.
5. da Silva, R. P., and S. Gordon. 1999. Phagocytosis stimulates alternative glycosylation of macrosialin (mouse CD68), a macrophage-specific endosomal protein. *Biochem. J.* **338:** 687–694.
6. O'Reilly, D., C. M. Quinn, T. El-Shanawany, S. Gordon, and D. R. Greaves. 2003. Multiple Ets factors and interferon regulatory factor-4 modulate CD68 expression in a cell type-specific manner. *J. Biol. Chem.* **278:** 21909–21919.
7. Gough, P. J., and E. W. Raines. 2003. Gene therapy of apolipoprotein E-deficient mice using a novel macrophage-specific retroviral vector. *Blood.* **101:** 485–491.
8. Pillai, M. M., B. Hayes, and B. Torok-Storb. 2009. Inducible transgenes under the control of the hCD68 promoter identifies mouse macrophages with a distribution that differs from the F4/80- and CSF-1R-expressing populations. *Exp. Hematol.* **37:** 1387–1392.
9. Pan, H., G. Mostoslavsky, E. Eruslanov, D. N. Kotton, and I. Kramnik. 2008. Dual-promoter lentiviral system allows inducible expression of noxious proteins in macrophages. *J. Immunol. Methods.* **329:** 31–44.
10. Ramprasad, M. P., W. Fischer, J. L. Witztum, G. R. Sambrano, O. Quehenberger, and D. Steinberg. 1995. The 94- to 97-kDa mouse macrophage membrane protein that recognizes oxidized low density lipoprotein and phosphatidylserine-rich liposomes is identical to macrosialin, the mouse homologue of human CD68. *Proc. Natl. Acad. Sci. USA.* **92:** 9580–9584.
11. Murphy, J. E., P. R. Tedbury, S. Homer-Vanniasinkam, J. H. Walker, and S. Ponnambalam. 2005. Biochemistry and cell biology of mammalian scavenger receptors. *Atherosclerosis.* **182:** 1–15.
12. Kurushima, H., M. Ramprasad, N. Kondratenko, D. M. Foster, O. Quehenberger, and D. Steinberg. 2000. Surface expression and rapid internalization of macrosialin (mouse CD68) on elicited mouse peritoneal macrophages. *J. Leukoc. Biol.* **67:** 104–108.
13. Sambrano, G. R., and D. Steinberg. 1995. Recognition of oxidatively damaged and apoptotic cells by an oxidized low density lipoprotein receptor on mouse peritoneal macrophages: role of membrane phosphatidylserine. *Proc. Natl. Acad. Sci. USA.* **92:** 1396–1400.
14. de Beer, M. C., Z. Zhao, N. R. Webb, D. R. van der Westhuyzen, and W. J. de Villiers. 2003. Lack of a direct role for macrosialin in oxidized LDL metabolism. *J. Lipid Res.* **44:** 674–685.
15. Malleret, G., U. Haditsch, D. Genoux, M. W. Jones, T. V. Bliss, A. M. Vanhoose, C. Weitlauf, E. R. Kandel, D. G. Winder, and I. M. Mansuy. 2001. Inducible and reversible enhancement of learning, memory, and long-term potentiation by genetic inhibition of calcineurin. *Cell.* **104:** 675–686.
16. Srinivas, S., T. Watanabe, C. S. Lin, C. M. William, Y. Tanabe, T. M. Jessell, and F. Costantini. 2001. Cre reporter strains produced by targeted insertion of *EYFP* and *ECFP* into the *ROSA26* locus. *BMC Dev. Biol.* **1:** 4.
17. Nagy, A., J. Rossant, R. Nagy, W. Abramow-Newerly, and J. C. Roder. 1993. Derivation of completely cell culture-derived mice from early-passage embryonic stem cells. *Proc. Natl. Acad. Sci. USA.* **90:** 8424–8428.
18. Park, C., S. Li, E. Cha, and C. Schindler. 2000. Immune response in Stat2 knockout mice. *Immunity.* **13:** 795–804.
19. Zhao, W., E. N. Cha, C. Lee, C. Y. Park, and C. Schindler. 2007. Stat2-dependent regulation of MHC class II expression. *J. Immunol.* **179:** 463–471.
20. Melillo, J. A., L. Song, G. Bhagat, A. B. Blazquez, C. R. Plumlee, C. Lee, C. Berin, B. Reizis, and C. Schindler. 2010. Dendritic cell (DC)-specific targeting reveals Stat3 as a negative regulator of DC function. *J. Immunol.* **184:** 2638–2645.
21. Chang, D. H., C. Angelin-Duclos, and K. Calame. 2000. BLIMP-1: trigger for differentiation of myeloid lineage. *Nat. Immunol.* **1:** 169–176.
22. Hendriks, W. L., H. van der Boom, L. C. van Vark, and L. M. Havekes. 1996. Lipoprotein lipase stimulates the binding and uptake of moderately oxidized low-density lipoprotein by J774 macrophages. *Biochem. J.* **314:** 563–568.
23. Song, L., and C. Schindler. 2004. IL-6 and the acute phase response in murine atherosclerosis. *Atherosclerosis.* **177:** 43–51.

24. Song, L., S. Bhattacharya, A. A. Yunus, C. D. Lima, and C. Schindler. 2006. Stat1 and SUMO modification. *Blood.* **108:** 3237–3244.

25. Bhattacharya, S., and C. Schindler. 2003. Regulation of Stat3 nuclear export. *J. Clin. Invest.* **111:** 553–559.

26. Plumlee, C. R., C. Lee, A. A. Beg, T. Decker, H. A. Shuman, and C. Schindler. 2009. Interferons direct an effective innate response to Legionella pneumophila infection. *J. Biol. Chem.* **284:** 30058–30066.

27. Jewell, N. A., T. Cline, S. E. Mertz, S. V. Smirnov, E. Flano, C. Schindler, J. L. Grieves, R. K. Durbin, S. V. Kotenko, and J. E. Durbin. 2010. Lambda interferon is the predominant interferon induced by influenza A virus infection in vivo. *J. Virol.* **84:** 11515–11522.

28. Martin, F. J., M. I. Gomez, D. M. Wetzel, G. Memmi, M. O'Seaghdha, G. Soong, C. Schindler, and A. Prince. 2009. Staphylococcus aureus activates type I IFN signaling in mice and humans through the Xr repeated sequences of protein A. *J. Clin. Invest.* **119:** 1931–1939.

29. Porter, D. W., L. L. Millecchia, P. Willard, V. A. Robinson, D. Ramsey, J. McLaurin, A. Khan, K. Brumbaugh, C. M. Beighley, A. Teass, et al. 2006. Nitric oxide and reactive oxygen species production causes progressive damage in rats after cessation of silica inhalation. *Toxicol. Sci.* **90:** 188–197.

30. Cassel, S. L., S. C. Eisenbarth, S. S. Iyer, J. J. Sadler, O. R. Colegio, L. A. Tephly, A. B. Carter, P. B. Rothman, R. A. Flavell, and F. S. Sutterwala. 2008. The Nalp3 inflammasome is essential for the development of silicosis. *Proc. Natl. Acad. Sci. USA.* **105:** 9035–9040.

31. Pernis, B., and F. Paronetto. 1962. Adjuvant effect of silica (tridymite) on antibody production. *Proc. Soc. Exp. Biol. Med.* **110:** 390–392.

32. Pernis, B. 2005. Silica and the immune system. *Acta Biomed.* **76 (Suppl. 2):** 38–44.

33. Landsman, L., and S. Jung. 2007. Lung macrophages serve as obligatory intermediate between blood monocytes and alveolar macrophages. *J. Immunol.* **179:** 3488–3494.

34. Rabinowitz, S. S., and S. Gordon. 1991. Macrosialin, a macrophage-restricted membrane sialoprotein differentially glycosylated in response to inflammatory stimuli. *J. Exp. Med.* **174:** 827–836.

35. Shiloh, M. U., J. D. MacMicking, S. Nicholson, J. E. Brause, S. Potter, M. Marino, F. Fang, M. Dinauer, and C. Nathan. 1999. Phenotype of mice and macrophages deficient in both phagocyte oxidase and inducible nitric oxide synthase. *Immunity.* **10:** 29–38.

36. Ninio, S., and C. R. Roy. 2007. Effector proteins translocated by Legionella pneumophila: strength in numbers. *Trends Microbiol.* **15:** 372–380.

37. Trinchieri, G., and A. Sher. 2007. Cooperation of Toll-like receptor signals in innate immune defence. *Nat. Rev. Immunol.* **7:** 179–190.

38. Hornung, V., F. Bauernfeind, A. Halle, E. O. Samstad, H. Kono, K. L. Rock, K. A. Fitzgerald, and E. Latz. 2008. Silica crystals and aluminum salts activate the NALP3 inflammasome through phagosomal destabilization. *Nat. Immunol.* **9:** 847–856.

39. Timmer, A. M., and V. Nizet. 2008. IKKbeta/NF-kappaB and the miscreant macrophage. *J. Exp. Med.* **205:** 1255–1259.

40. Sambrano, G. R., S. Parthasarathy, and D. Steinberg. 1994. Recognition of oxidatively damaged erythrocytes by a macrophage receptor with specificity for oxidized low density lipoprotein. *Proc. Natl. Acad. Sci. USA.* **91:** 3265–3269.

41. Huynh, K. K., E. L. Eskelinen, C. C. Scott, A. Malevanets, P. Saftig, and S. Grinstein. 2007. LAMP proteins are required for fusion of lysosomes with phagosomes. *EMBO J.* **26:** 313–324.

42. Barois, N., B. de Saint-Vis, S. Lebecque, H. J. Geuze, and M. J. Kleijmeer. 2002. MHC class II compartments in human dendritic cells undergo profound structural changes upon activation. *Traffic.* **3:** 894–905.

43. Chow, A., D. Toomre, W. Garrett, and I. Mellman. 2002. Dendritic cell maturation triggers retrograde MHC class II transport from lysosomes to the plasma membrane. *Nature.* **418:** 988–994.